Naval Research Laboratory
Washington, DC 20375-5000

NRL Memorandum Report 6278

Applications of Layered Synthetic Microstructures in Vacuum Ultraviolet and Soft X-Ray Grating Spectrometers

J. C. RIFE

Synchrotron Radiation Research Group
Condensed Matter and Radiation Sciences Division

September 14, 1988

SECURITY CLASSIFICATION OF THIS PAGE

REPORT DOCUMENTATION PAGE

Form Approved
OMB No 0704-0188

1a REPORT SECURITY CLASSIFICATION UNCLASSIFIED	1b RESTRICTIVE MARKINGS
2a SECURITY CLASSIFICATION AUTHORITY	3 DISTRIBUTION / AVAILABILITY OF REPORT Approved for public release; distribution unlimited.
2b DECLASSIFICATION / DOWNGRADING SCHEDULE	
4 PERFORMING ORGANIZATION REPORT NUMBER(S) NRL Memorandum Report 6278	5 MONITORING ORGANIZATION REPORT NUMBER(S)
6a NAME OF PERFORMING ORGANIZATION Naval Research Laboratory 6b OFFICE SYMBOL (If applicable) Code 4600	7a NAME OF MONITORING ORGANIZATION
6c ADDRESS (City, State, and ZIP Code) Washington, DC 20375-5000	7b ADDRESS (City, State, and ZIP Code)
8a NAME OF FUNDING / SPONSORING ORGANIZATION Office of Naval Research 8b OFFICE SYMBOL (If applicable) Code 01111	9 PROCUREMENT INSTRUMENT IDENTIFICATION NUMBER
8c ADDRESS (City, State, and ZIP Code) Arlington, VA 22217	10 SOURCE OF FUNDING NUMBERS PROGRAM ELEMENT NO: 63221C; PROJECT NO; TASK NO; WORK UNIT ACCESSION NO

11 TITLE (Include Security Classification)
Applications of Layered Synthetic Microstructures in Vacuum Ultraviolet and Soft X-Ray Grating Spectrometers

12 PERSONAL AUTHOR(S)
Rife, J.C.

13a TYPE OF REPORT	13b TIME COVERED	14 DATE OF REPORT (Year, Month, Day)	15 PAGE COUNT
Interim	FROM 3/88 TO 7/88	1988 September 14	49

16 SUPPLEMENTARY NOTATION

17 COSATI CODES			18 SUBJECT TERMS (Continue on reverse if necessary and identify by block number)
FIELD	GROUP	SUB-GROUP	

19 ABSTRACT (Continue on reverse if necessary and identify by block number)

Potential multilayer grating applications for the wavelength region from 6 to 350Å are discussed. Multilayer bandwidth and efficiency as affected by stack construction as well as the effects of roughness and corrections to Bragg's law are considered. Grating performance is reviewed with attention to the limitations to high resolving powers and spectral purity in fabrication and instrument design. Combined multilayer grating performance is discussed for both broad and narrow band coatings. Designs for; (a) 10-40Å (0° resolving power spectrograph, (b) 6-60Å scanning monochromator, and (c) a 170Å or 45Å region, medium resolution, broad-band spectrograph/monochromator are explored.

1,500

(Abstract)

20 DISTRIBUTION / AVAILABILITY OF ABSTRACT	21 ABSTRACT SECURITY CLASSIFICATION
☒ UNCLASSIFIED/UNLIMITED ☐ SAME AS RPT ☐ DTIC USERS	UNCLASSIFIED
22a NAME OF RESPONSIBLE INDIVIDUAL J.C. Rife	22b TELEPHONE (Include Area Code) (202) 767-4654 22c OFFICE SYMBOL Code 4606

DD Form 1473, JUN 86 Previous editions are obsolete SECURITY CLASSIFICATION OF THIS PAGE

S/N 0102-LF-014-6603

CONTENTS

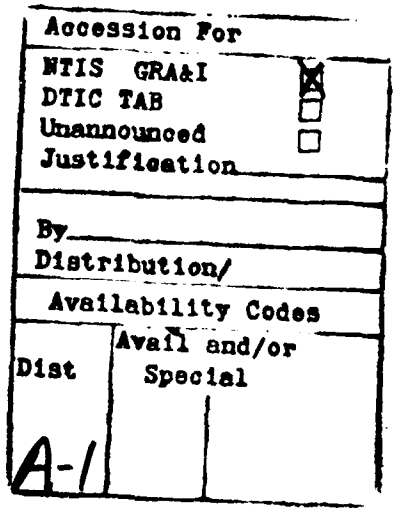

APPLICATIONS OF LAYERED SYNTHETIC MICROSTRUCTURES IN VACUUM ULTRAVIOLET AND SOFT X-RAY GRATING SPECTROMETERS

1. Introduction

In the past 10 years, new capabilities in thin film deposition and lithography have brought fresh ideas into ultraviolet and soft x-ray instrumentation. Layered synthetic microstructures or multilayers, transmission gratings, and zone plates have found applications in a wide variety of fields including astronomy, microscopy, plasma diagnostics, and synchrotron radiation. Interest in multilayers, in particular, has grown phenomenally since the first materials combinations were developed that formed smooth, durable interfaces. Clearly, the extension of normal incidence optics designs to the spectral domain of grazing incidence optics as well as the ability to engineer synthetic crystals to serve in the crystal range were strong inducements. Spiller[1] and Barbee[2] have reviewed the techniques of multilayer fabrication as well as calculations and measurements of multilayer performance. A forthcoming conference will concentrate on various x-ray multilayer applications in diffractometers, monochromators, and spectrometers.[3]

This paper will focus on the promise of multilayer-coated grating instrumentation where the multilayer enhances the reflectivity and the grating provides the resolution. There are a number of potential advantages of multilayer-coated gratings. First, as noted above, multilayers permit new wavelength-angle regions to be exploited. Fig. 1 shows critical angle behavior

Manuscript approved July 14, 1988.

where $\cos\theta_c = n_a(\lambda)$ and reflectance falls rapidly to less grazing angles or shorter wavelength for the low Z and high Z coatings of aluminum and gold; n_a is the index of refraction and θ_c is the critical grazing angle. Also shown is Bragg's law

$$n\lambda = 2D\sin\theta \qquad (1)$$

for a number of crystals typically used in spectrometers, where n is the order, λ is the wavelength, D is the spacing between crystal planes, and θ is the grazing angle. The crystal region is limited to shorter wavelengths by the availability of large 2D spacing materials. In fact, the largest 2D spacing materials such as Langmuir-Blodgett films, mica, or even KAP are not robust enough for high heat load applications such as synchrotron radiation. The cross-hatched area shows the large region where multilayers, which also obey Bragg's law, can permit new types of designs. In particular, normal incidence designs with more intense, stigmatic images and normal incidence on plate or detector can be brought to the wavelength range from 30 to 350 Å. Access to larger grazing angles of incidence and reflection also means that higher grating orders and consequently higher resolving powers can be obtained. Multilayer gratings can also serve as synthetic crystals of medium resolving power, spanning the difficult spectral range between grating and crystal instruments, and even bringing higher resolving powers to the long wavelength end of the crystal region where resolving powers

are limited by absorption. There are a number of problems for the application of multilayer coated gratings. These include: corrections to Bragg's law which are stronger at long wavelengths; reduced efficiency due to substrate and interfacial roughness particularly at shorter wavelengths; coherence of grating and multilayer diffraction; and multiple diffraction planes.

This paper is directed to monochromator and spectrograph design, but will point to what design and fabrication limits exist for multilayers. Part 2 will discuss multilayer performance. Part 3 will cover issues of grating instrument design. And Part 4 will consider the constraints of combined multilayer-grating performance and examine three potential classes of vacuum ultraviolet and soft x-ray multilayer grating instruments: a) narrow band high resolving power (10^5) spectrographs using blazed gratings in high order; b) wide-range, narrow-band, medium resolving power (10^3) scanning monochromators using blazed gratings; and c) simple, broad-band, normal-incidence, medium resolving power spectrographs or monochromators.

2. Multilayer performance

To first order, multilayers act as Bragg reflectors following Equa. 1 with typical θ-2θ behavior. The standard VUV

multilayer is constructed of absorptive layers of thickness T_a having optical constants n_a and k_a alternating with relatively transparent spacer layers of thickness T_s and optical constants n_s and k_s. Each bilayer forms a period, $D = T_a + T_s$, and a total of N periods forms the stack. Selection of materials for the absorber and spacer layers depends on the spectral behavior of the optical constants desired and practical considerations of fabrication and material compatibility. Absorption edges, particularly in the spacer layer, dramatically reduce the optical constant contrast necessary for high reflectance. For wavelengths as long as 100-600Å, large absorption for all materials limits useful stack thickness. Minimum practical 2D spacings are on the order of 30Å; so higher multilayer orders must be used to attain normal incidence at shorter wavelengths. Layer materials must form smooth, stable interfaces. They must not interdiffuse or roughen, during or after deposition. These constraints have led to a few standard coatings such as ReW-C, W-C, or Mo-Si[4]; with others less frequently used; and still more possibilities not yet explored. Two techniques predominate the fabrication of multilayers; thermal or, more specifically, e-beam evaporation [5,6] and sputtering[2]. Both techniques have their advantages, but higher reflectivity has been obtained with sputtered coatings.[6] A recent conference has dealt with the synthesis of multilayers, especially in the area of thin film growth.[7]

Ideal multilayer performance is well understood. A number of

papers specifically address the calculation of properties.[8,9,10] In general, those papers focus on calculation techniques derived from the dynamical theory of x-ray diffraction or Fresnel's laws. With the optical constants fully taken into account, the methods are, in fact, equivalent. Care must be taken, however, in adapting some of the formulae, which were developed under the approximation of $n_a, n_s \doteq 1$ and $k_a, k_s \doteq 0$. Such assumptions are reasonable for the x-ray region, but are not good at longer wavelengths. The potential for long wavelength VUV multilayers has been addressed recently by Hunter.[11] Multilayers are characterized by: a maximum reflectance , R_m; a bandwidth, angular acceptance, or resolving power (all equivalent) of $\Delta\lambda$, $\Delta\theta$, or $\lambda/\Delta\lambda$; or a total integrated reflectance, R_t (in radians). These features are affected by: the spectral behavior of the optical constants; polarization of the radiation; stack construction; and non-ideal performance due to nonuniformities and roughness.

Peak reflectance values for multilayers typically range up to 10-20% in normal incidence, rising to higher values at more grazing angles. Reflectance, of course, varies with polarization, leading to a very strong rejection of the p-polarized component at what is essentially Brewster's angle. Efficient x-ray polarizers based on this behavior have been designed and constructed.[12] For an ideal multilayer at fixed θ, peak reflectance depends on the effective number of periods contributing, N_{eff}. When the multilayer is absorption limited or

the total number of periods in the stack, N, is less than the penetration depth of the radiation, the kinematic theory of diffraction is appropriate; and $R_m \propto N^2$. For a small number of layers, R_m is maximized by making the absorber layers as thick as possible or $\gamma = T_a/D = 0.5$. For a larger number of layers, R_m is increased by reducing γ, and thus increasing the transmission of each individual absorber layer, so that there is a larger number of periods contributing. Eventually, of course, absorption in the spacer limits R_m. A multilayer is extinction limited in short wavelength regions where absorption is very small and the radiation is mostly reflected. In this regime, the dynamical theory is more appropriate; and R_m falls below N^2. In either regime, R_m can be optimized for a stack of identical periods by finding the best γ. Allowing γ to vary within the stack can yield an improved R_m for a small number of layers, as shown by the reflectance optimized deposition of Spiller[4]; but for a large number of layers the approaches converge to a fixed γ.[13]

The bandwidth, resolving power, or angular acceptance of multilayers is equivalently affected by stack construction. Multilayer resolving powers are roughly given by $\lambda/\Delta\lambda \sim nN_{eff}$; typical maximum values are 100 at the shortest wavelengths. With large angular acceptance and bandwidth, multilayers offer great flux advantages with continuum sources over applications using crystals, where resolving powers range from 10^3 to 10^4 and rocking curve widths range from 10^2 to 10 arc-seconds in the spectral region from 10Å to 1Å. Multilayers have also been

optimized for instruments with broad bandwidth in the long wavelength region (100-300Å and 300-600Å bands).[9,14] Narrow-band optimization while highly desirable for a variety of spectroscopic applications is constrained by absorption in the spacer layer. In the long wavelength region, bandwidths as narrow as 70Å at 450Å and 10Å at 200Å have been obtained by Meekins.[14] For shorter wavelengths where k_s is small and n_s - 1, Kozhevnikov and Vinogradov[10] have shown that the upper limit of resolving power is controlled by absorption in the spacer layer and is given by

$$\frac{\lambda}{\Delta\lambda} = \frac{\sin^2\theta}{2n_s k_s} \qquad (2)$$

With layer thicknesses practically limited to values greater than 5Å, the resolving power limit, given optimal optical constants, should be about 200 at 125Å rising to about 1000 at 25Å. Real devices, however, yield resolving powers of no more than 100-300, even at the shortest wavelengths. One fabrication constraint is lateral D spacing uniformity which is at best on the order of 0.3% across several cm for sputtered multilayers.[15] Attempts to attain high resolving power are usually based on low Z, low optical constant contrast couples; but also recent efforts have been made to construct "Fabry-Perot" devices. These devices are either a pair of multilayers separated by a thick spacer layer[16]

or a distributed form, a multilayer stack where specific absorber layers are replaced by additional spacer layers[17]. Results are, as in Equa. 2, constrained by absorption in the spacer layer and indicate resolving powers of 400 can be attained for real devices at 1.85Å. Higher resolving powers demand using vacuum as a spacer layer. Part 4 of this paper will suggest how higher resolving powers could be obtained with multilayer-coated diffraction gratings.

Fig. 2 shows a typical example of multilayer performance which illustrates some of the features noted above. The reflectance or rocking curves were calculated applying Fresnel's laws at each interface in the thin film stack, which provides the full electromagnetic solution.[18] Optical constants were obtained from the compilation of Henke et al.[19] The figure shows s, p, and average reflectance for 100 period, 60Å 2D spacing tungsten/carbon multilayers at 45Å versus grazing angle θ. The reflectances are calculated for two tungsten absorber to D spacing ratios, γ=0.25 in Fig. 2a and γ=0.5, equal thicknesses, in Fig. 2b. Fig. 2 displays the expected strong suppression of p-polarized reflectance near Brewster's angle for both multilayers. Reflectance and angular width or bandwidth are also clearly shown to be controlled by penetration depth or, more particularly, by absorption in the tungsten layers. The γ=0.5 multilayer of Fig 2b with twice the tungsten thickness of the γ=0.25 multilayer in Fig. 2a has an N_{eff} of about 50 compared to an N_{eff} of about 100 in Fig. 2a and, as a result, an equivalently

lower reflectance and broader angular width. The lineshapes of both are similar showing long $1/\theta^2$ Lorentzian tails while the γ=0.25 multilayer shows secondary interference maxima.

Corrections to Bragg's law are also evident in Fig. 2. The arrows show the uncorrected angular location. Bragg' law, corrected for refraction alone, is

$$n\lambda = 2D\sin\theta_1 \sqrt{1 - \frac{1 - n_a^2}{\sin^2\theta_1}} \quad . \qquad (3)$$

where θ_1 is the corrected Bragg grazing angle and n_a is an averaged index of refraction. This is a standard x-ray crystal formula, but for absorbing materials an additional correction must be made, as noted by Rosenbluth and Lee[20], yielding a new angle θ_2. At wavelengths above 100 Å, θ_2-θ can be as large as one and one-half degrees with the correction for absorption alone (θ_2-θ_1) being about 10-20% of the full correction unless the wavelength is close to an absorption edge (and on the transparent side), in which case, the correction for absorption can be as great as 80-90% of the full correction. As indicated previously, the calculations for Fig. 2 include refraction and absorption and so show the full correction. The smaller correction for Fig. 2a versus 2b is expected since the tungsten 1-n_a is by selection significantly larger than for carbon. Deviations from the Bragg angle could apparently present a problem for multilayer-grating

designs which require strict θ-2θ behavior, particularly at longer wavelengths where the correction is as large as several degrees. But, in fact, the loss in reflectance is not as large as might be expected. Fig. 3 shows the FWHM and Bragg correction in degrees versus wavelength for the 100 period, γ=0.5 W/C multilayer of Fig. 2b. The correction remains on the order of only 1/2 of the FWHM across a broad range from 55 to 30Å. Greater losses, indeed, will occur at shorter wavelengths where the correction rises to an angular value as large as the FWHM. Note that the ratio of correction to FWHM even improves in the region of the carbon K edge around 44Å, although the actual s-polarized reflectance drops considerably from 17.9% at 45Å to 6.9% at 40Å. The ratio of correction to FWHM for the γ=0.25 multilayer is similar. Other multilayer materials should display comparable behavior but need to be considered individually.

The major obstacle in obtaining the maximum reflectance of multilayers, particularly at short wavelengths, is interfacial roughness. Various authors have treated the subject.[6,21,22,23] Scattering from rough surfaces can be divided into incoherent scattering from facets whose lateral extent is larger than the coherence length of the radiation (approximately the first Fresnel zone) or coherent scattering from roughness whose lateral extent is less than the coherence length. The former is, in fact, figure or slope error and gives rise to a spread in 2θ. For multilayers, $\Delta\theta$ would effectively increase while R_t would remain about the same. Coherent scattering is dependent on the

rms roughness, σ, and the lateral periodicity.[24] The angular dependance can be modeled as a superposition of gratings of various groove density. The angular dependence and polarization effects will not be discussed here. But assuming that each interface has the same roughness and that the multilayer is not extinction limited, the magnitude in the specularly or Bragg reflected beam is given by a prefactor multiplying the ideal multilayer reflectance, in essence, a Debye-Waller factor squared

$$(DWF)^2 = e^{-4\left\{\frac{2\pi\sigma\sin\theta}{\lambda}\right\}^2} \qquad (4)$$

Indeed, reduced R_m due to interfacial roughness, interdiffusion, and non-accumulating thickness errors all follow the above relationship. While R_m drops, $\Delta\theta$ stays essentially constant since the number of effective layers stays the same. Reduced reflectance at individual interfaces does not only lead to enhanced scattering but also to enhanced transmission; so that when a multilayer is extinction limited, increased roughness leads to somewhat lower R_m but also reduced $\Delta\theta$. Spiller and Rosenbluth have shown that a simple DWF prefactor multiplying the reflected amplitude at each layer with losses going into increased transmission predicts the reflectance losses whether the multilayer is absorption or extinction limited.[16] In those

cases where the roughness varies from layer to layer within a stack, the effect is to lower R_m but also to broaden $\Delta\theta$, similar to the effect of accumulating thickness errors. Note that, in general, higher orders are affected more strongly. Inserting Bragg's law into Equa. 4,

$$(DWF)^2 = e^{-4\left\{\frac{2\pi\sigma n}{2D}\right\}^2} \qquad (5)$$

the reduction goes like the first order prefactor to the n^2 power. Also note that for given multilayer and order, the reduction is independent of λ or θ and dependent only on σ and D. For essentially undiminished peak reflectance, this demands $\sigma \leq D/10n$. Such a requirement is an inducement to push short wavelength multilayer designs certainly to lower orders but also to larger 2D spacings and thus away from normal incidence. Some substrates can be polished to σ levels of 5Å; while the best superpolishes are on the order of 3Å. For a σ of 3Å and the minimum 2D of 30Å, Equa. 4 predicts a prefactor of 0.20 in first order which becomes 0.002 in second order. This, of course, is a worst case result; overestimating the effects for those multilayers which are extinction limited at short x-ray wavelengths ($\lambda \leq 8$ Å).[15] In those cases and at least for R_t, dynamical theory would apply and the factor of 4 in Equa. 4 could

be replaced by a factor of 2 in the perfect crystal limit, resulting in prefactor values of 0.45 in first order and 0.042 in second order. The effects of roughness on the efficiency of multilayer-coated gratings is not clear at this time. The grating model of roughness, certainly, predicts that shorter wavelengths will be scattered at angles closer to the specular direction. Clearly calculations and measurements need to be made. More will be discussed in Part 4.

A final note on spectral purity with regard to the application of multilayers to grating instruments. For continuum sources, higher orders could be a problem; but at longer wavelengths, at least, the orders separate in angle due to the Bragg corrections; and with the ability to engineer stack construction, higher orders can be relatively suppressed with judicious choice of γ. Scattered light, although due to roughness and connected with lower reflectance, should be relatively less than with single layer coatings, since $R_m \alpha N^2$ but the scattered light is only proportional to N.[16]

3. Grating Performance and Mounts

Progress in VUV grating instrumentation is driven predominately by spectroscopic needs in plasma diagnostics, astronomy, and synchrotron radiation. General ultraviolet

grating performance and typical instrument mounts have been reviewed by Sampson.[25] Most recently, Michette[26] has reviewed soft x-ray applications of diffraction gratings, zone-plates, and multilayers. A comprehensive discussion of the theory, fabrication, and use of diffraction gratings is given by Hutley[27] while Maystre, Neviere, and Petit have compared measurements and full electromagnetic calculations of grating efficiency[28]. Recent astronomical instrumentation has appeared in several conference proceedings.[29] New developments in synchrotron radiation instrumentation have been reviewed by Johnson[30] and by Gluskin[31]. One of the prime advantages of multilayer coatings will be to bring normal incidence or Littrow designs to shorter wavelengths. The requirement of grazing angles at wavelengths shorter than 300 Angstroms due to critical angle effects leads to enhanced aberrations and, in particular, to increased astigmatism in Rowland circle mounts. Normal incidence will provide more intense, stigmatic images and lower f/numbers for a given grating size. Less obvious but more attractive is the potential for higher resolution. Of course, the drawback for spectrometers is reduced bandwidth. This section will discuss grating resolution, efficiency, and fabrication limits, all with the potential of multilayer-coated grating applications and for high resolving powers in mind.

The standard grating equation takes the forms

$$m\lambda = d(\sin\alpha - \sin\beta) \qquad (6i)$$

$$\text{or} \quad = d(\cos i - \cos r) \qquad (6ii)$$

$$\text{or} \quad = 2d \sin\phi \sin\theta \qquad (6iii)$$

where m is the order (+ inside and - outside), d is the grating period, α and β are the angles of incidence and diffraction relative to the grating normal (β changes sign when on the same side of the normal as the incoming light), and i and r are the corresponding grazing angles of the incoming and diffracted light relative to the grating surface. In the final equation, ϕ is the blaze angle and θ is the grazing angle on a blaze facet. Equa. 6iii is appropriate for the on-blaze operation of blazed gratings where the peak diffracted intensity occurs at an angle $\delta = 2\phi$ from zero order or the specularly reflected beam. This form reveals the equivalency with Bragg's law, where here the D spacing is $d\sin\phi$, the spacing between blaze facets. It is also clearly the equation of choice when considering applications using a Bragg reflecting multilayer overcoating. Unblazed gratings can be cast in the same form with $\phi = \delta/2$ and $\theta = i + \delta/2$ where δ is now variable. Considering the scattering origins of diffraction and the effects of groove profile, Equa 6iii is, in fact, the most physical form of the grating equation.

Dispersion and resolving power given by the dispersion alone can be derived from Equa. 6. The angular dispersion in the diffracted beam is

$$\frac{dr}{d\lambda} = \frac{m}{d \sin r} \qquad (7)$$

This leads to a resolving power determined by dispersion of

$$\left\{ \frac{\lambda}{d\lambda} \right\}_d = \frac{f_r}{s_r \sin r} \frac{m \lambda}{d} \qquad (8i)$$

or

$$= \frac{2 f_r}{s_r} \frac{1}{\cot\phi + \cot\theta} \qquad (8ii)$$

where dr, the angle subtended, has become s_r/f_r for instruments with an exit slit or recording element of width s_r at a focal distance of f_r. 8ii is given for inside order. Outside order differs by a minus sign on $\cot\theta$. Extension of the following comments to outside order is straightforward, albeit reversed. The resolving power given by Equa. 8 is, of course, limited by physical optics to a maximum resolving power determined by the order and the number of grooves coherently illuminated, N_c.

$$\left\{ \frac{\lambda}{d\lambda} \right\}_m = m N_c \qquad (9)$$

N_c, in turn, is given by the projected width on the grating of the first Fresnel zone of the light diffracted from the entrance slit of width s_i. The maximum resolving power for an underfilled grating in inside order, then, becomes

$$\left\{ \frac{\lambda}{d\lambda} \right\}_m = 0.91 \frac{f_i}{s_i \sin i} \frac{m\lambda}{d} \qquad (10i)$$

$$\text{or} \qquad = 0.91 \frac{2f_i}{s_i} \frac{1}{\cot\phi - \cot\theta} \qquad (10ii)$$

where f_i is the entrance slit to grating distance and the factor 0.91 comes from a modified Rayleigh criterion.[32] Note that the resolving power in 8ii and 10ii is a function of incidence angle and diffraction direction alone and not the order m. This applies if the grating is underfilled with coherent radiation. If overfilled, the maximum resolving power is proportional to m and the number of grating grooves independent of angle. The highest resolving powers are achieved in Littrow and at grazing incidence whether under or overfilled, as will be discussed below.

Attaining the highest resolving powers in the UV and soft x-ray regions demands minimizing optic figure error, surface roughness, and mount aberrations and also pushing the limits of critical angle effects, orders, and grating groove density. Fig. 4 shows resolving power versus wavelength for Equas. 8i and 10i above, and the present maxima set by modern grating and crystal monochromators. All the grating instruments shown operate with 1000-2000 g/mm gratings. The highest resolving powers of 300,000 to 400,000 are obtained in 3rd or 4th order in

the spectral region from 800-2000Å with the Eagle mount of the Rowland circle.[33,34] The best resolving powers achieved at shorter wavelengths are all in first order and are 35,000-30,000 at 160-120 Å with a variable line spaced plane grating[35] and 3000-1000 from 100 to 16 Å with plane[36], toroidal[37], and spherical[38] grating monochromators. Below 16 Å, two broad rocking curve crystals, Beryl and Quartz are shown with resolving powers of 3000 to 10,000 , exceeding present grating instruments in that spectral range. The two lines in Fig. 4 represent Equas. 8i or 10i for 2 and 12 meter Rowland circle spectrometers with m = 1, a 1000 g/mm grating, and a typical minimum slit size of 10μ assumed. Since f_r=Rsinr and f_i=Rsini for Rowland spectrometers, the coefficients f_r/s_rsinr and f_i/s_isini become R/s_r and R/s_i or simply R/s because the entrance slit is imaged 1:1. Clearly, larger R/s is desirable; but s is limited by aberrations and detector size to 10-40 μ (typical limits: film, 10-12 μ; and channelplates or linear detector arrays, 20-40 μ); while R is often restricted by the practical consideration of laboratory size and budget; and R/s limited by vibration. Vibration, of course, would not be a limitation for unaveraged, short-pulse measurements. One of the advantages of more grazing incidence in Rowland or other such focussing designs is smaller overall length while preserving large values of R. The envelope of highest resolving power in Fig.4 is evidently set by the linear dependance on the order-wavelength product. To achieve higher resolving powers at shorter wavelengths demands higher orders.

But attainment of higher resolving powers below 300 Å is constrained by the requirement of smaller angles of diffraction and thus lower orders and larger groove spacings due to the drop off of reflectance above critical angles, which are progressively shallower at shorter wavelengths.

An additional perspective on resolving power is shown in Fig. 5 which plots the resolving power given by Equas. 8ii and 10ii versus the grazing angle on the groove facet for a number of blaze angles. This is most appropriate for fixed focal length instruments such as the grating/crystal monochromator (GCM)[39,40] that operate with crystals or with gratings always on blaze or for multilayer-coated gratings with an equivalent θ-2θ response. For Fig. 5, $2f_r/s_r$ is assumed to be the same as $2f_i/s_i$ and equal to 4×10^5 (e.g., 10 meter focal length with 50μ slits). This presumes the off-axis optics can be figured to a slope error of 1 arc second or better, a value at or exceeding state of the art. Fig. 5 shows that Equas 8ii and 10ii, for a given blaze angle, ϕ, are equal at normal incidence, in the Littrow condition (θ = 90 degrees). At shallower angles in inside order, the maximum physical resolving power rises and the resolving power set by dispersion falls off, limiting the resolution. Note that for a given ϕ, the dispersion resolving power has no solution below θ=ϕ since the grazing angle on the grating goes to 0°. Correspondingly, the maximum resolving power goes to infinity, limited by the real size of the grating. Unlike Rowland circle mounts, grating focussing is a factor in these fixed focal length

instruments; but this phenomena does not appear in Fig. 5. The entrance slit image is reduced at the exit slit by a factor $\sin(\theta-\phi)/\sin(\theta+\phi)$ so that resolving power can be maintained or increased by decreasing s_r as long as figure errors and aberrations permit. In outside order, the curves in Fig. 5 for Equas. 8ii and 10ii would be reversed. In that case, entrance slit magnification would increase with dispersion, but resolving power would be restricted by coherent resolving power. Increased resolution would necessitate reducing s_i. Fig. 5, besides showing the flat resolving powers and large spectral ranges available at small ϕ in inside order to instruments like the GCM, also makes clear the severe limitation that critical angle effects impose on resolving power and the great advantage in resolving power in Littrow with θ=90 degrees and with large ϕ. Indeed, the highest resolving powers are attained in Littrow in Eagle or echelle[41] spectrometers. Echelle spectrometers attain $>10^5$ resolving powers with coarse gratings (~ 10 g/mm and well defined blaze) in high orders (~ 500) so that a large spectral range is covered over a small angular spread. Note that for Littrow mounts with an overfilled grating, $\lambda/d\lambda$ is given by $2W\cos i/\lambda$ where W is the grating width. For a given wavelength and W the resolving power is a function of angle only and is highest at grazing incidence with the largest specular to diffracted light deviation, δ, and groove density can be anything. Low groove densities, although yielding a well defined blaze profile, imply high orders which restrict the free spectral

range of observation. The free spectral range, $d\lambda$, or the largest bandwidth which doesn't overlap the same bandwidth in an adjacent order is determined by

$$\left\{ \frac{\lambda}{d\lambda} \right\}_{fsr} = m \qquad (11)$$

Overlapping orders in echelle instruments are typically separated by a cross dispersing element. In general, multilayer coated grating instruments would permit operation at larger angle of diffraction with higher orders and/or finer grating spacings and would allow shifting of the lines or resolving power envelope in Fig. 4 rigidly to the left, that is, to shorter wavelength. Multilayer grating applications to GCM-type instruments or using the Littrow mount will be discussed in Part 4.

Broad and narrowband multilayer coatings can be applied to the great variety of grating forms to achieve higher UV and soft x-ray efficiencies and resolving powers. Pushing the limits will require careful consideration of grating surface figure, groove, placement accuracy, and groove profile. Gratings are typically fashioned by ruling or holographically. Ruled gratings are made by drawing a diamond stylus across a soft metal surface in a ruling engine. Modern ruling engines are interferometrically controlled and grooves are ruled to a precision of 0.6Å and better. Groove placement accuracy is on the order of 10Å[42], but significant spectral improvement has been observed where coma correction for a Seya mount required groove spacing variation in a range of ±1Å across 50mm[43]. Such varied line-space, ruled

gratings offer great potential in aberration correction and focussing for normal incidence and grazing incidence instruments.[44] Grooves for gratings in general can be blazed to angles as small as one degree and ruling densities can be as high as 3600-4800 g/mm, although they are more typically 600-2400 g/mm. Due to plastic flow, diamond wear, and other factors, the blazed groove profile is not triangular and is somewhat rough. The cusp formed at the top of the groove is inverted in plastic replicas for a more well-defined blaze. Holographic gratings can have more accurately placed grooves. They are fabricated by exposing a photoresist to a laser interference pattern and can be made with groove densities up to 6000 g/mm. Ion-etching or other processes can then form the master. Laminar, sinusoidal, or blazed groove profiles can be formed; but blazed gratings usually require a transparent substrate. Holographic gratings with laterally curved grooves can provide certain types of aberration correction, such as a flat focal field for a Rowland circle mount.

Groove placement tolerances[27] depend on application but are more stringent for higher orders. Highest resolving powers for a given grating width demand meeting Rayleigh's criterion or wavefront errors of less than $\lambda/4$, although Stroke[45] quotes an upper limit of tolerable "extended" wavefront aberration of $\lambda/10$. A maximum wavefront error of $\lambda/4$ means that groove spacing error, δd, must be

$$\delta d < \frac{\lambda}{8 \cos i} \qquad (12i)$$

or in Littrow

$$\delta d < \frac{d}{4 m} \qquad (12ii)$$

Clearly grazing and grazing Littrow mounts require more groove accuracy than normal incidence mounts and wavefront errors of $>\lambda/4$ must be tolerated at wavelengths of less than 80Å for ruled gratings and for shorter wavelengths with holographic gratings. An equivalent constraint is the wavefront error produced by figure error, coating error, or, in general, height irregularities, δh, on the grating surface. To yield a wavefront error less than $\lambda/4$[27]

$$\delta h < \frac{\lambda}{8 \sin i} \qquad (13)$$

Note that this δh would apply only across the width of grating necessary to provide the resolution desired, and is forgiving in grazing incidence (θ would substitute for i on a blaze facet). Departure from groove straightness or fan is another grating groove error which for Littrow is on the order of 3d/m. Periodic ruling errors or ghosts have almost been eliminated in modern gratings; but since the intensity of ghosts relative to zero order intensity is

$$\frac{I_{ghost}}{I_{0order}} = \left\{ \frac{\pi\, m\, \delta d}{d} \right\}^2 \qquad (14i)$$

ghosts can be a greater problem at higher orders. For Equa 14i to be less than 10^{-6} in Littrow,

$$\delta d < \frac{2\, d}{10^3\, \pi\, m} \qquad (14ii)$$

More troublesome for standard gratings are random ruling errors which contribute focussed stray light or grass. Grass is proportional to

$$\frac{I_{grass}}{I_{spec}} = \left\{ \frac{4\pi\, \overline{\delta d}\, \cos i}{} \right\} \qquad (15i)$$

where $\overline{\delta d}$ is the mean groove spacing error. To achieve less than one percent grass

$$\overline{\delta d} < \frac{\lambda}{120\, \cos i} \qquad (15ii)$$

Holographic gratings generally have fewer ghosts and less grass due to their more accurate groove placement, although groove irregularities can occur during photoresist development. Hunter has discussed grass and, in particular, compares grass from ruled and holographic gratings.[46] Ghosts and scattered light from ruled and holographic gratings as well as grass from echelles in

100th order have been measured by Mount and Fastie.[47]

Grating efficiency in the UV is determined by polarization effects, coating reflectance, and groove profile. The full electromagnetic theory[28] has been quite successful in predicting grating efficiencies. Polarization anomalies, as such, can be ignored with UV gratings because the wavelengths and groove densities fall in the scalar regime with $\lambda<d/5$. Overall scalar grating efficiency is given by the product of coating reflectance and groove profile efficiency.[28,48] This is found valid for incidence angles up to at least 40°. Fig. 6 shows the groove efficiency versus λ/h, where h is the groove height, for the three ideal, standard profiles; blazed or triangular, sinusoidal, or laminar.[49] Blazed gratings are most efficient, reaching almost 100% at λ/h of 2. This is obviously linked to the Bragg-like formulation of the grating equation, Equa. 6iii, since the groove height for blazed gratings is essentially $d\sin\phi$. That is, blazed gratings act exactly like crystals with d spacing $d\sin\phi$. A rule of thumb for real blazed grating efficiency predicts an on-blaze efficiency of 40% of coating reflectance.[50] Laminar gratings are usually designed with a step height to give destructive interference of light scattered from the top and bottom of the groove in zero and even orders and, at the same time providing constructive interference in odd orders. For small deviations of diffraction direction and zero order, this condition in fact results in a first order peak of constructive interference at $\lambda/h=4$, as shown. Since the highest scattering

efficiency for laminar gratings is in the specular direction, their efficiency cannot approach that of a blazed grating. But surface roughness of the plateau of the laminar grating groove can be much better than the facet of the blazed grating because the original flat polish on the plateau does not need to be altered during grating fabrication. Accurate efficiency calculations for laminar gratings must also include considerations of groove shadowing and plateau transparency.[51] The peak efficiency of the sinusoidal profile is closer to the laminar peak but is located at $\lambda/h=3.4$, between the blazed and the laminar efficiency curves in wavelength. The sinusoidal profile offers a range of angles of incidence to the incoming radiation.

4. Multilayer-grating performance and instrument designs

There have been very few published measurements or theoretical calculations of multilayer-coated gratings. Keski-Kuha[52] deposited a 5 layer Ir/Si multilayer with a D spacing of ~ 180Å onto a 5000 groove/mm sinusoidal holographic grating. She observed a factor of three improvement in efficiency at 304Å, whereas the reflectance of the simple

multilayer alone at 304Å times the expected scalar efficiency would suggest a factor of twelve improvement. Jark[53] applied a 3 period Au/C multilayer with 182Å D spacing to a 1200 groove/mm blazed grating with 1.5° blaze. He observed a 10 times improvement in efficiency over a similar gold coated grating at 50 and 100 Å at grazing angles where the efficiency is falling off (substantially off blaze). He noted that second order is unenhanced and so relatively suppressed. Hawryluk et al[54] fabricated 60000Å and 2000Å d spacing gold stripe gratings on top of a Mo/Si multilayer with 115Å D spacing. The devices were intended to serve as soft x-ray laser end-mirror/coupling elements. At 208Å, they measured zero order efficiencies of 8 and 2% for the large and small period gratings and first order efficiencies of .76 and .6%; these efficiencies were 66, 25, 95 and 142% of calculated values. Barbee[55] examined the performance of two types of multilayers on 500 groove/mm laminar gratings in a two-crystal monochromator with the first element a multilayer and the second a grating coated with the identical multilayer. At 8.24Å, he looked at a 120 period Rh/C multilayer with 39.4Å D spacing at a 6° grazing angle; and at 114Å he inspected a 40 period Rh/C multilayer with 80 Å D spacing at a 50° grazing angle. He saw as many as thirteen diffraction peaks in both the grating scan with detector fixed (rocking curve) and in a detector scan with multilayer grating fixed. The zero order flux was measured to be 30% that of a straight multilayer/multilayer pair while the "1st order" flux was 23%.

Vidal et al[49] calculated multilayer-grating efficiencies for sinusoidal, laminar, and blazed gratings with multilayer coatings of Mo/Si and Nb/Al in the wavelength regions of 125-145Å and 240-360Å respectively. They demonstrated that the scalar theory is sufficiently close to the full differential formalism for practical purposes as long as the angle of incidence, α, is less than 40°. At 45° they saw a rigid shift in efficiency peak between the differential and scalar calculations. Their calculations for all grating types were for a λ/h of 4, the peak of laminar grating efficiency. Clearly, more basic measurements and further calculations need to be made to map out the limitations of multilayer coated grating devices.

Two potential multilayer grating applications stand out; first, a narrow-band, multilayer-coated blazed grating to operate in medium or high resolution in a scanning monochromator or in high orders in Littrow and second, a broad-band multilayer grating to operate in low orders and in near-normal incidence. The following discussion will cover the narrow-band type first, a more demanding application, which will serve to illustrate multilayer grating performance issues. This will be succeeded by a short look at broad-band multilayer grating performance and finally by consideration of several instrument possibilities using both types. The designs are presented for exploratory purposes only; multilayer grating efficiencies and resolving powers have been presumed which need experimental verification.

Coating a blazed grating with a properly optimized, narrow-

band multilayer coating yields a diffraction element which has a high reflectivity over a limited wavelength/diffraction angle range. Combining Bragg's law of Equa. 1 with the grating equation of Equa. 6iii yields the necessary matching condition

$$\frac{D}{n} = \frac{d\sin\phi}{m} \qquad (16)$$

The resolving power is set by the grating to be mN_c, but equivalently, the combination can be viewed as a synthetic crystal (asymmetrically cut) with N_c blaze facets of m periods each contributing of a total number of sampled layers or crystal planes of mN_c. In practice, the number of periods deposited or contributing can be greater or less than m; $d\sin\phi$ defines the "D" spacing of the grating "crystal" planes. Most likely, multilayer D would be determined by measuring the grating $d\sin\phi$. To achieve high efficiency the D spacing should be accurate to D/N_{eff}. Sputtered multilayers have a depth and lateral (over several cm) uniformity of <0.3%.[14] If the $\lambda/d\lambda$ bandwidth of the multilayer, given by N_{eff}, is designed to be equal to m, the multilayer bandwidth will match the free spectral range, reducing the problem of overlapping spectral orders, particularly where the grating and multilayer orders differ. Greater order suppression can be achieved with larger N_{eff}, but care must be taken, especially at shorter wavelengths, to avoid lower efficiencies due to the Bragg correction as shown in Figs. 2 and 3.

Adjustments to the D spacing could match the corrected Bragg and blaze angles, but this would be optimal at only one wavelength. As noted in Part 2, the Bragg correction is tolerable for a large wavelength region at longer wavelengths; and so matching would be best done at shorter wavelengths. Multilayer grating efficiency as a function of diffraction angle would be determined, in part, by the single slit diffraction pattern with a angular FWHM of approximately λ/d. In terms of bandwidth in the dispersed spectrum, this becomes (from Equa 7 without including groove shadowing)

$$\left\{ \frac{\lambda}{d\lambda} \right\}_s = \frac{m \cos\phi}{\sin r} \qquad (17)$$

Another consideration for multilayer gratings is the possibility of having multiple diffraction planes. These could result in diffraction features from what would be, in effect, higher index planes of the synthetic crystal/multilayer grating. Efficiency would depend a number of factors such as the single slit diffraction width since the multilayer grating "atoms" are, in fact, small plane facets.

Fabrication errors in multilayer gratings constrain the resolving powers and efficiencies, particularly at the shorter wavelengths. For high resolving powers a focussing system is required. Putting aside design questions of a curved grating substrate or separate focussing mirrors, Rayleigh's criterion giving the highest resolution for a given width grating demands

that the wavefront error be less than $\lambda/4$. As shown by Equa. 12, this puts strong restrictions on groove placement errors which have to be 2Å at λ=16Å and half as small at λ=8Å. One Ångstrom is not within the capabilities of the best ruling engines, and so holographic gratings may be preferred. Figure error or height irregularities, δh, also contribute to wavefront error and constrain resolving power. Equa. 13 and Bragg's law imply that $D \geq 4\delta h$ or that given the state of the art of optical fabrication is, at best, 5 to 10Å deviation of surface figure from a given ideal, D spacings must be $\geq$ 20-40Å. This limits standard high resolution, normal incidence designs to wavelengths larger than 20Å. It applies to micro-irregularities or roughness as well, but the effects on efficiency can be gauged more quantitatively from Equas. 4 and 5. Those relationships predict 1/3 remaining in the specular beam at a rms roughness to D spacing ratio, σ/D, of $\simeq$ 1/6. The roughness, therefore, must be less than 5Å for a multilayer with a 2D of 60Å. This is difficult to achieve with flat surfaces much less on the facets of blazed gratings. Ion-etched holographic gratings may be preferred over other blazed types because of lower roughness. But, in general, a flat blaze facet is difficult to achieve with holographic gratings.[27] Other possibilities are moving to coarser gratings (and correspondingly higher orders, m) which have a higher quality, flatter blaze, or perhaps using anisotropically etched silicon gratings.[56] Certainly fabrication questions such as multilayer coating uniformity across the blaze facet are also open. For short

wavelengths, roughness may force designs to non-normal incidence to obtain sufficient efficiency.

The constraints on lower resolution, broad-band multilayer gratings are less restrictive; and, as mentioned, several have been fabricated. These devices would use a wide rocking curve multilayer coating and aim to reach moderate to high resolving powers in low orders. For short wavelength applications, the roughness problem could be relieved by using laminar gratings as substrates which can have very smooth plateaus. Unfortunately the facets put the multilayer efficiency peak in the zero order direction, so efficiency cannot be as high as blazed multilayer gratings and the interference between groove top and bottom cannot be put to full use to enhance odd orders because the bottom of the grooves would be relatively rough. Sinusoidal multilayer gratings might offer higher efficiencies at larger δ due to the range of grazing angles presented; but, again, roughness would be a limitation at short wavelength.

Multilayer grating performance suggests three classes of instruments to explore. The first are spectrographs that use narrow-band, "synthetic crystal", blazed multilayer gratings to achieve up to 10^5 resolving powers for wavelengths as short as 10-40Å. The second are scanning monochromators which also use narrow-band, blazed multilayer gratings but with moderate 10^3-10^4 resolving powers and operate on-blaze over a wide angular and wavelength range. The final class adapts standard normal-incidence, stigmatic grating mounts for use with broad-band

multilayer gratings. Each of these classes will be discussed in turn. Fig. 7 shows the mounts that will be considered, some in more than one class. Other more exotic possibilities which offer potential for new focussing arrangements but a more complicated and less precise grating will not be discussed here. These include the on-blaze, variable spacing cylinder grating monochromator of Aspnes[57] or other designs using variable groove spacing grating focussing such as proposed by Hettrick and Bowyer[58] or Cash[59] as well as Fresnel zone plate monochromators.

Design of a multilayer grating spectrograph to attain 10^5 resolving powers for wavelengths as short as 10-40Å places the greatest demands on grating and multilayer fabrication. From the discussion of grating instruments and resolving powers, it is clear that to reach such resolving powers in a reasonable size instrument a Littrow configuration with a large blaze angle grating and small grazing angles on the grating surface is necessary. This is, in fact, the standard approach to reach very high resolution in the visible or near-visible. But the Littrow configuration with multilayer grating would have only a limited on-blaze spectral range of high efficiency. Three possible mounts are depicted in Fig. 7; (a), the Czerny-Turner, (b) the Eagle, and (c) the Monk-Gilleson. A fourth possibility, the echelle spectrograph (e.g. Harrison[41]) has not been illustrated because of its similarity to the Czerny-Turner spectrometer and the added complexity of a cross-dispersing spherical grating (in place of the second spherical mirror, M2) for order sorting.

Order sorting is naturally supplied by the multilayer in any event, although another order sorting mechanism could be required for a wider spectral range with broader band coatings. All three of the mounts shown are normal incidence ones and so offer an essentially stigmatic image. The resolving powers of the three mounts are limited by other aberrations and, at the sort wavelengths, primarily by fabrication errors. The fabrication errors will be discussed later. But the errors favor fewer optical surfaces and those that can be figured more accurately. Aberrations in the Eagle mount are low and have been considered by Namioka[33]. While it has a single optical element, that element is a spherical grating. The Czerny-Turner and Monk-Gilleson mounts both use plane gratings which are more precisely made. The Monk-Gilleson offers two surfaces, but is normally considered for more moderate resolution instruments because of severe coma. The coma can, however, be compensated against astigmatism at one wavelength.[60,61] Coma can also be compensated by hyperbolic grating grooves or an off-axis ellipsoid mirror in place of the spherical mirror[62], but this is adding more potential fabrication errors. The Czerny-Turner mount has small astigmatism and coma which can be compensated against each other at a given wavelength and well tolerated for a relatively large range across the spectrograph plate.[63,64] The Czerny-Turner mount would be favored for its low aberrations and plane grating; but, again, the fabrication errors of three optical surfaces have to be tolerated. The two spherical mirrors could be coated with

narrow-band or broad-band multilayers to match the grating coating. Broad-band coatings of all elements would allow larger spectral coverage on the plate or operation as a wider range monochromator.

Fig. 8 shows the resolving power, derived from Equas. 8 and 10 , for fully Littrow (θ=90°) spectrometers versus the grazing angle of incidence on the grating, i. The resolving power is basically a simple function of tani. Maximum and dispersion resolving powers are the same in the fully Littrow case. Resolving power is shown for instruments of 1,2,5 and 10 meter focal lengths with a practicable 25μ slit size. Also plotted on the abscissa is the order-wavelength product for a 1000 groove/mm grating and the resultant order for a wavelength of 20Å. For a typical 2 meter instrument with ϕ=65° blaze angle and so i=25°, the resolving power would be 3.4×10^5. With a 1000 groove/mm grating, this would result in operation in 900th order at 20Å. For a real instrument, i would need to be on the order of 87° or 93° for sufficient lateral separation of optical elements. Note that 87° yields a i=22° for inside order, and 93° is associated with i=28° for what is effectively outside order in the standard Czerny-Turner mount. Either case would result in only a minor lowering of resolving power from the Littrow configuration.

The primary limitation to resolving power at the shorter wavelengths would be wavefront error, ghosts or satellites, and scattered light (grass). For the 2 meter instrument mentioned above at 20Å, Equas. 12 and 13 would require a groove placement

accuracy of better than 2.7Å and height variations of less than 2.5Å to obtain better than $\lambda/4$ wavefront error and full resolving power. It is not clear if the groove accuracy required is within the capabilities of interferometrically controlled ruling engines; they certainly are within a factor of four. The height restrictions would apply to blank figure, facet flatness, and multilayer uniformity; and is likely out of the reach of fabrication methods. The best approach is to tolerate whatever errors cannot be reduced by designing for higher resolving powers than required. Ghosts and grass in the observed spectrum may present an even greater problem since they are proportional to the grating order squared. For ghosts to be $<10^{-3}$ and grass $<10^{-2}$ of spectral features, periodic ruling errors and random ruling errors must be <0.1Å, for a 1000 g/mm grating in 1000th order. This is ≃ 1/10 to 1/100 of the ruling accuracy of modern ruling engines. To bring the accuracies within ruling range would require operation in 30th to 300th order and correspondingly finer ruling densities of >3000 g/mm. The blaze facet flatness suffers at higher ruling densities, and very few, if any, gratings have been ruled at groove densities higher that 4800 g/mm. The required groove placement accuracy for 1000 g/mm gratings may be achieved with holographic gratings. Efficiency at these shorter wavelengths would also be strongly reduced by roughness. Equas. 4 and 5 predict a roughness of only 5Å rms at a wavelength of 20Å would yield an efficiency 0.005% that of a perfectly smooth multilayer. This would dissuade applications

that do not demand such high resolutions and cannot tolerate such low efficiency. Again, measurements of actual short wavelength multilayer grating performance are needed to bear all the estimates of resolving power, background, and efficiency out.

The second class of potential multilayer grating instruments is composed of scanning monochromators that operate on-blaze to match the multilayer θ-2θ condition and in low orders with moderate 10^3-10^4 resolving powers. Hunter has reviewed a variety of on-blaze mounts.[46] Many of the on-blaze instruments suffer the experimental drawback of a moving exit slit. Fig. 7d shows the GCM, an on-blaze, fixed exit-slit, scanning monochromator that operates with a pair of gratings, a mirror and a grating, or a pair of crystals as diffraction elements, G1 and G2, in the region of collimated light between a pair of grazing incidence paraboloidal mirrors, M1 and M2. As it is implemented at the National Synchrotron Light Source, f_i=f_r=10,000mm and s_i=s_r=800μ so that with 2D=60Å, n=1, ϕ=5°, d=5000Å, m=15, and a multilayer coated mirror-grating pair, the GCM wavelength range would be 6Å to 60Å with corresponding grating grazing angles, i, of 1° to 82° and a constant resolving power of $\doteq$ 2200. This resolving power equals or exceeds the highest resolving powers to date in that wavelength region as shown in Fig. 4. Resolving powers to 5000 and above could be achieved at larger blaze angles, ϕ, and higher orders, m; but the spectral range would be cut off on the short wavelength side. The fabrication error tolerance for this class of instruments is reduced over that for the very high resolving

power spectrographs but still presents strong limitations on grating precision. For the GCM, grazing incidence at the shorter wavelengths strongly relaxes the tolerance for heights deviations. Heights errors would have to be less than 46Å to 7.2Å over the 6Å to 60Å range of the monochromator. While this is practicable, groove placement errors would have to be 0.8Å to 6.4Å in the spectral range 6Å to 60Å to meet the designed resolving power. Although ruled gratings are nearly precise enough, this probably demands a holographic grating. Ghosts and grass also still remain a problem even though the design calls for only 15th order. Periodic ruling errors would have to be less than 3.3Å for $<10^{-3}$ ghosts or less than 0.1Å for $<10^{-6}$ ghosts. Random ruling errors would have to be <0.05Å at 6Å, <0.7Å at 50Å, and <9Å at 58Å. Such errors again argue for the groove placement precision of a holographic grating. As mentioned previously, the multilayer roughness on the blaze facet would have to be less than 5Å rms for no less than a 1/3 drop in efficiency. It is likely that efficiencies will be lower, perhaps much lower. Measurements need to be made to more clearly outline the performance limitations.

The final class of potential multilayer grating instruments has the most relaxed fabrication limits. It involves adapting normal-incidence, stigmatic, scanning monochromators or spectrographs to VUV and soft x-ray wavelengths with broad-band multilayer coatings operating in low orders (m=1-4). The thrust is to provide, a simple and possibly compact instrument with

moderate resolving powers (10^3) and reasonable bandwidth ($\sim\lambda/m$) in the spectral regions from 100 to 400Å or perhaps 25 to 100Å. Narrower bandwidth coatings could be used for higher efficiency but patchy coatings of different 2D spacings or multiple gratings would be needed for wide spectral coverage. One advantage of lower order instruments is the possibility of using laminar gratings with very smooth facets although the facets are wrongly directed for highest efficiency. Figs. 7 a, c, and e are all possible candidates for this class. The Czerny-Turner and Monk-Gilleson mounts would be altered to operate with gratings in more normal incidence with smaller blaze angles. Both mounts have the advantage of plane gratings but more optical surfaces. The normal-incidence Rowland circle mount is simple and offers a single reflecting surface. It will be considered as the test case although the analysis should apply to all. A 2 meter, normal-incidence Rowland circle spectrograph or monochromator with $s_i=s_r=25\mu$, $i=87°$, and $\delta=2°$ so that $\phi=1°$ for blazed gratings, 2D=175Å, d=5000Å, n=1, and m=1 would have a resolving power of 2800 (from Equa. 8ii) and reasonable efficiency over a single slit diffraction range of approximately 100 to 250Å or the bandwidth of the multilayer coating, whichever is smaller. Higher resolving powers at the same wavelength could be attained at larger blaze angles, ϕ; but this would require smaller d/m ratios, that is, smaller groove spacings or higher orders. A 45Å 2D multilayer coating could be applied to yield the same resolving power but in the 4th grating order, m. Resolution

could be maintained for groove placement errors as great as 415Å at 175Å or 105Å at 45Å while height deviations from ideal must be less than 22Å at 175Å or 6Å at 45Å. These can be achieved. Reasonable levels of ghosts and grass are also within or close to fabrication limits. Periodic ruling errors must be less than 50Å (12.6Å) for ghosts to be $<10^{-3}$ at 174Å (45Å) or more stringently less than 1.6Å (0.4Å) for ghosts to be $<10^{-6}$ at 174Å (45Å). Random ruling errors must be less than 28Å (7Å) for grass to be less than 1% at a wavelength of 174Å (45Å). Again, holographic gratings are more desirable.

5. Conclusion

Multilayer gratings have the potential to bring normal-incidence, high-intensity, stigmatic imaging spectrographs and monochromators to wavelengths from 13 to 350Å. High resolution Littrow spectrographs, medium resolution scanning monochromators, and lower resolution spectrographs and monochromators can all be envisioned but demands on grating and surface figure are high because of the short wavelengths and high orders. Holographic gratings offer the best hope to meet the groove placement accuracy required, but the question of facet flatness remains. Measurements need to be made, particularly to verify estimates of efficiency due to roughness, actual resolving powers, and the backgrounds of ghosts and grass.

REFERENCES

1. Eberhard Spiller, Mat.Res.Soc.Symp., 56 , 419-433 (1986).

2. Troy W. Barbee, Jr. , Opt. Engr.,25, 898-915 (1986).

3. SPIE Conference on X-ray Multilayers for Diffractometers, Monochromators, and Spectrometers, San Diego, August 1988.

4. T.W. Barbee Jr, S. Mrowka, and M.C. Hettrick, Applied Optics, 24, 883-886 (1985).

5. E. Spiller, A. Segmuller, J. Rife, and R.P. Haelbich, Appl.Phys.Lett., 37, 1048-1050 (1980).

6. M.P. Bruijn, thesis, Vrije Universeteit Te Amsterdam (1986); M.P. Bruijn, P. Chakraborty, H.W. van Essen, J. Verhoeven, and M.J. van der Wiel., Opt. Engr., August 1986; M.P. Bruijn, W.J. Bartels, P.Chakraborty, H.W. van Essen, J. Verhoeven, and M.J. Weil, in SPIE 563, 182-194 (1985).

7. "Multilayers: Synthesis, Properties, and Nonelectronic Applications", Materials Research Society Symposium Proceedings, Volume 103 (1988).

8. J.H. Underwood and T.W. Barbee, in Low Energy X-Ray Diagnostics- 1981, D.T. Attwood and B.L. Henke, eds., AIP Conf.Proc. No.75, AIP, New York, 170-178 (1981).

9. Alan E. Rosenbluth and J.M. Forsyth in Low Energy X-Ray Diagnostics-1981, D.T. Attwood and B.L. Henke, eds., AIP Cong. Proc. No. 75, AIP, New York, 280-285 (1981).

10. I.V. Kozhevnikov and A.V. Vinogradov, Physica Scripta, T17, 137-145 (1987).

11. W.R. Hunter, SPIE 869, (1988). to be published.

12. A. Khandar and P. Dhez, SPIE, 563, 158-163 (1985).

13. J.F. Meekins, R.G. Cruddace, and H. Gursky, Applied Optics 25,2757 (1986).

14. J.F. Meekins, R.G. Cruddace, and H. Gursky, to be published in Applied Optics 86,87?

15. T.W. Barbee Jr., private communication.

16. T. Barbee Jr. and J.H. Underwood, Opt. Comm., 48, 161-166 (1983).

17. M.P. Bruijn, J. Verhoeven, M.J. van der Wiel, and W.J. Bartels, Opt. Engr., 26, 679-684 (1987).

18. Computer program developed by W.R. Hunter.

19. B.L. Henke, P. Lee, T.J. Tanaka, R. Shimabukuro, and B.K. Fujikawa, Atom. Data Nucl. Data Tables, 27, 1 (1982).

20. Alan E. Rosenbluth and Ping Lee, Appl.Phys.Lett. 40, 466-468 (1982).

21. Eberhard Spiller and Alan E. Rosenbluth, SPIE, 563, 221-236 (1985).

22. M.P. Bruijn, Thesis, Vrije Universiteit Te Amsterdam, 1986; M.P. Bruijn, W.J. Bartels, P. Chakraborty, J.W. van Essen, J. Verhoeven, and M.J. van der Weil, SPIE, 563, 182-194 (1985)

23. J.V. Gilfrich, D.B. Brown, D.L. Rosen, and R.L. Freitag in Materials Research Society Symposium on Multilayers: Synthesis, Properties, and Non-electronic Applications (1987).

24. H. Hogrefe and C. Kunz, Applied Optics, 26, 2851 (1987).

25. J.A.R. Samson, Techniques of Vacuum Ultraviolet Spectroscopy, John Wilwy & Sons, Inc., New York (1967).

26. A.G. Michette, Optical Systems for Soft X-Rays, Plenum Press New York (1986).

27. M.C. Hutley, Diffraction Gratings, Academic Press, New York (1982).

28. D. Maystre, M. Neviere, and R. Petit, in Electromagnetic Theory of Gratings, Topics in Current Physics, Vol. 22, Springer-Verlag, Berlin, 159-225 (1980).

29. SPIE, 563 (1985) and 688 (198*).

30. R.L. Johnson in Handbook on Synchrotron Radiation, Vol 1b, ed by E. Koch, North-Holland, Amsterdam, 173-260 (1983).

31. E.S. Gluskin, Nucl. Instr. and Meth. A261, 60-65 (1987).

32. J.E. Mack, J.R. Stehn, and Bengt Edlen. JOSA, 22, 245-264 (1932).

33. T. Namioka, JOSA, 49, 446-460 and 460-465 (1959).

34. K. Ito, T. Sasaki, T. Namioka, K. Ueda, and Y. Morioka, Nucl.Instr. and Meth., A246, 290-293 (1986).

35. M.C. Hettrick, J. H. Underwood, P.J. Batson, and M.J. Eckart, Applied Optics, 27, 200-202 (1988).

36. H. Petersen, Nucl. Instr. and Meth., A246, 260-263 (1986).

37. F.J. Himpsel, Y. Jugnet, D.E. Eastman, J.j. Donelon, D. Grimm, G. Landgren, A Marx, J.F. Morar, C. Oden, R.A. Pollak, J. Schneir, and C.A. Crider, Nucl. Instr. and Meth., 222, 107-110 (1984).

38. C.T. Chen, Nucl. Instr. and Meth., A256, 595-604 (1987).

39. W.R. Hunter, R.T. Williams, J.C. Rife, J.P. Kirkland, and M.N. Kabler, Nucl. Instr. and Meth., 195, 141-153 (1982).

40. J.C. Rife, W.R. Hunter, and R.T. Williams, Nucl. Instr. and Meth., A246, 252-255 (1986).

41. G.R. Harrison, JOSA, 39, 522-528 (1949), G.R. Harrison J.E. Archer, and J.C. Camus, JOSA, 42, 706-712 (1952).

42. B. Bach, Hyperfine Inc., private communication.

43. T. Harada, T. Kita, M. Itou, and H Taira, Nucl. Instr. and Meth., A246, 272-277 (1986).

44. M.C. Hettrick, SPIE, 560, 96-108 (1985).

45. G.W. Stroke, JOSA, 51, 1321-1339 (1961).

46. W.R. Hunter in Spectrometric Techniques, Vol. IV, ed by G.Vanasse, Academic Press, New York, 63-180 (1985).

47. G.H. Mount and W.G. Fastie, Applied Optics, 17, 3108-3116 (1978).

48. E.G. Loewen and M. Neviere, Applied Optics, 17, 1087-1092 (1978).

49. B. Vidal, P. Vincent, P. Dhez, and M. Neviere, SPIE, 563, 142-149 (1985).

50. W.R. Hunter and J.C. Rife, Applied Optics, 23, 293-299 (1984).

51. M. Neviere, J. Flamand, and J.M. Lerner, Nucl. Instr. and Meth., 195, 183-189 (1982).

52. R. A. M. Keski-Kuha, Applied Optics, 23, 3534-3537 (1984).

53. W. Jark, Optics Communications, 65, 201-205 (1986).

54. A.M. Hawryluk, N.M. Ceglio, D.G. Stearns, K. Danzman, M. Kuhne, P. Muller, and B. Wende, SPIE 688, 81-90 (1986).

55. Barbee MRS paper

56. D.R. Ciarlo and D.E. Miller, SPIE, 688, 163-170 (1986).

57. D.E. Aspnes, JOSA, 72, 1056 (1982).

58. M.C. Hettrick and S. Bowyer, Applied Optics, 22, 3921 (1983).

59. W.C. Cash Jr., Applied Optics, 22, 3971 (1983).

60. M. Seya, T. Namioka, and T. Sai, Sci. of Light, 16, 138-157 (1967).

61. D.J. Schroeder, JOSA, 60, 1022-1026 (1970).

62. M.V.R.K. Murty, JOSA, 52, 768-773 (1962).

63. A.B. Shafer, L.R. Megill, and L. Droppelman, JOSA, 54, 879-887 (1964).

64. J. Reader, JOSA, 59, 1189-1196 (1969).

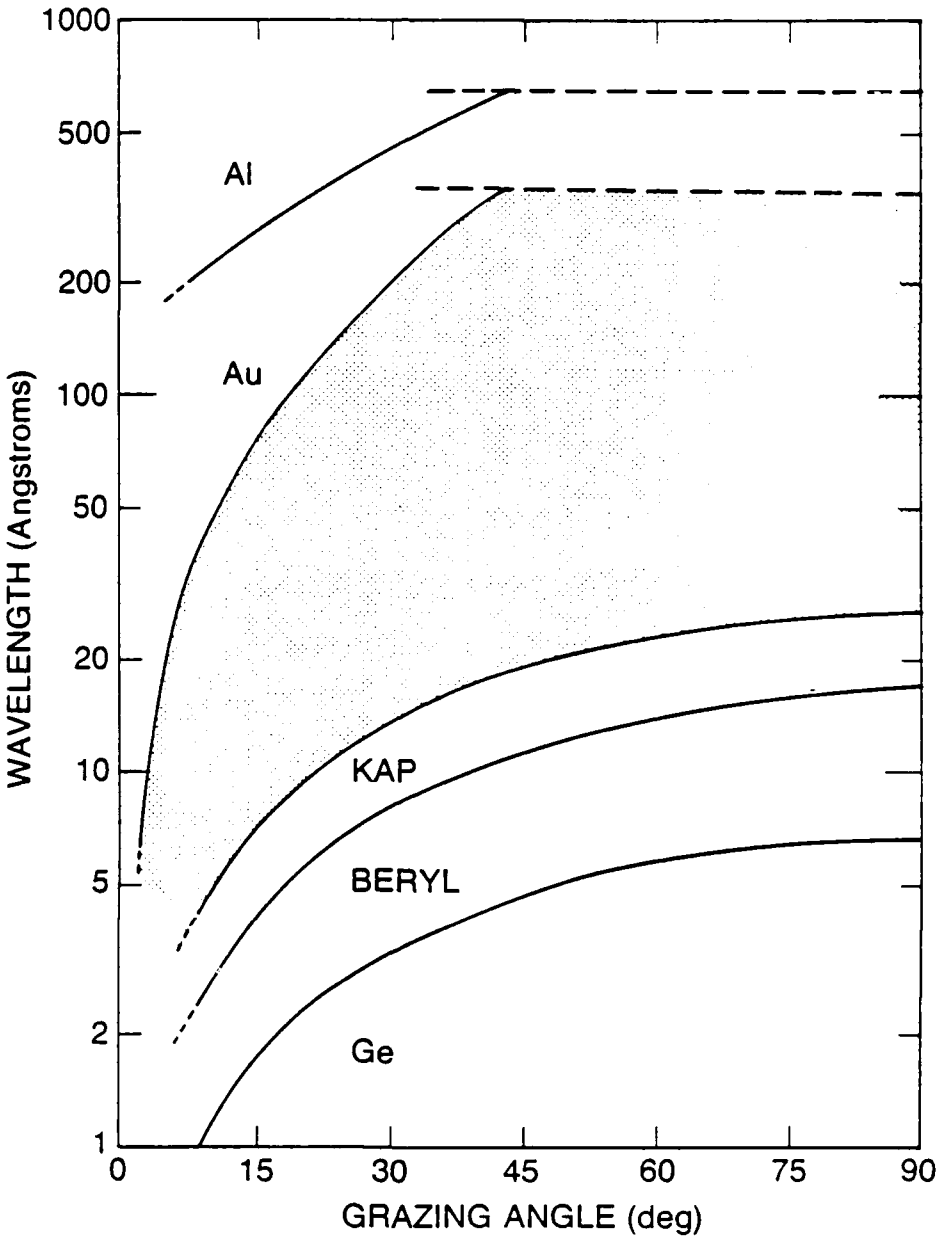

Fig. 1. Wavelength versus critical grazing angle for aluminum and gold where reflectance falls dramatically at less grazing angles or shorter wavelength. Dashed lines are outside critical angle regime and serve only to indicate wavelength where normal incident reflectance falls below 10%. Bragg conditions for the standard, large D spacing planes of KAP, Beryl, and germanium are also shown. Shaded region is newly accessible through multilayer designs.

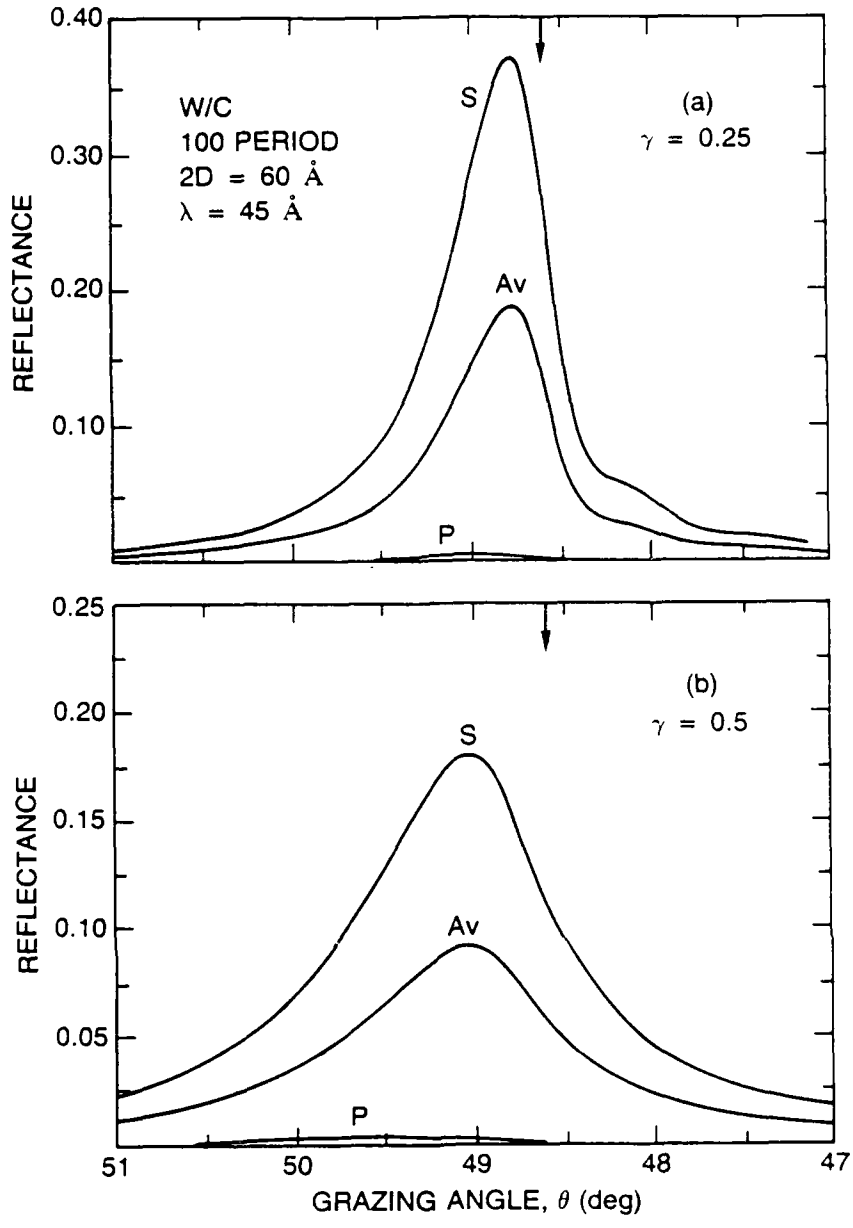

Fig. 2. Calculated s,p,and average reflectance versus grazing angle for a 30Å D spacing, 100 period W/C multilayer at λ=45Å. (a) absorber thickness to D spacing ratio γ=0.25, (b) γ=0.5, equal absorber and spacer thicknesses. The arrows denotes the angular position predicted by Bragg's law.

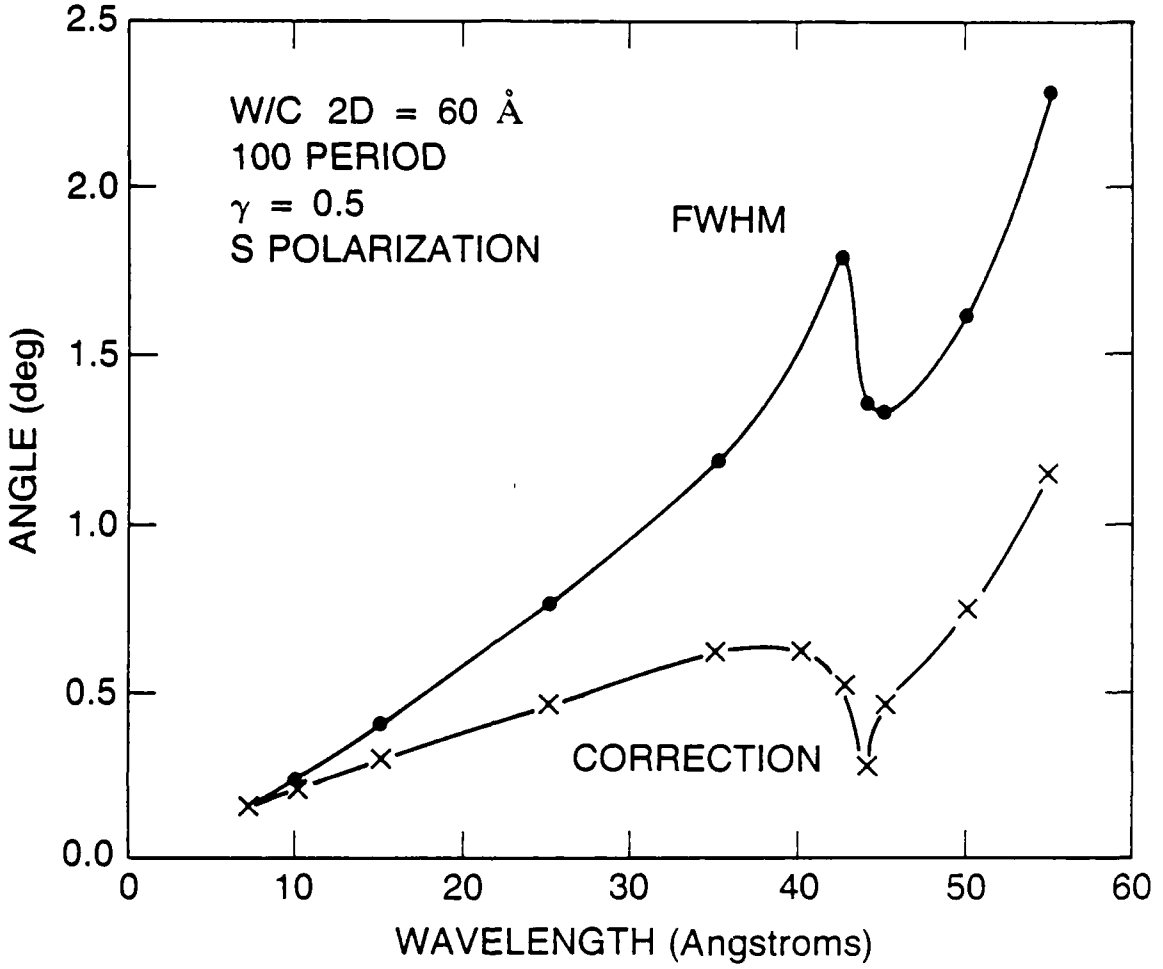

Fig. 3. Spectral dependance of the angular FWHM and angular shift or correction to pure Bragg law behavior of the reflectance of the multilayer of Fig. 2b, W/C 100 period, 60Å 2D spacing. The carbon K edge appears prominently at 44Å. Lines drawn between calculated points are for clarity only.

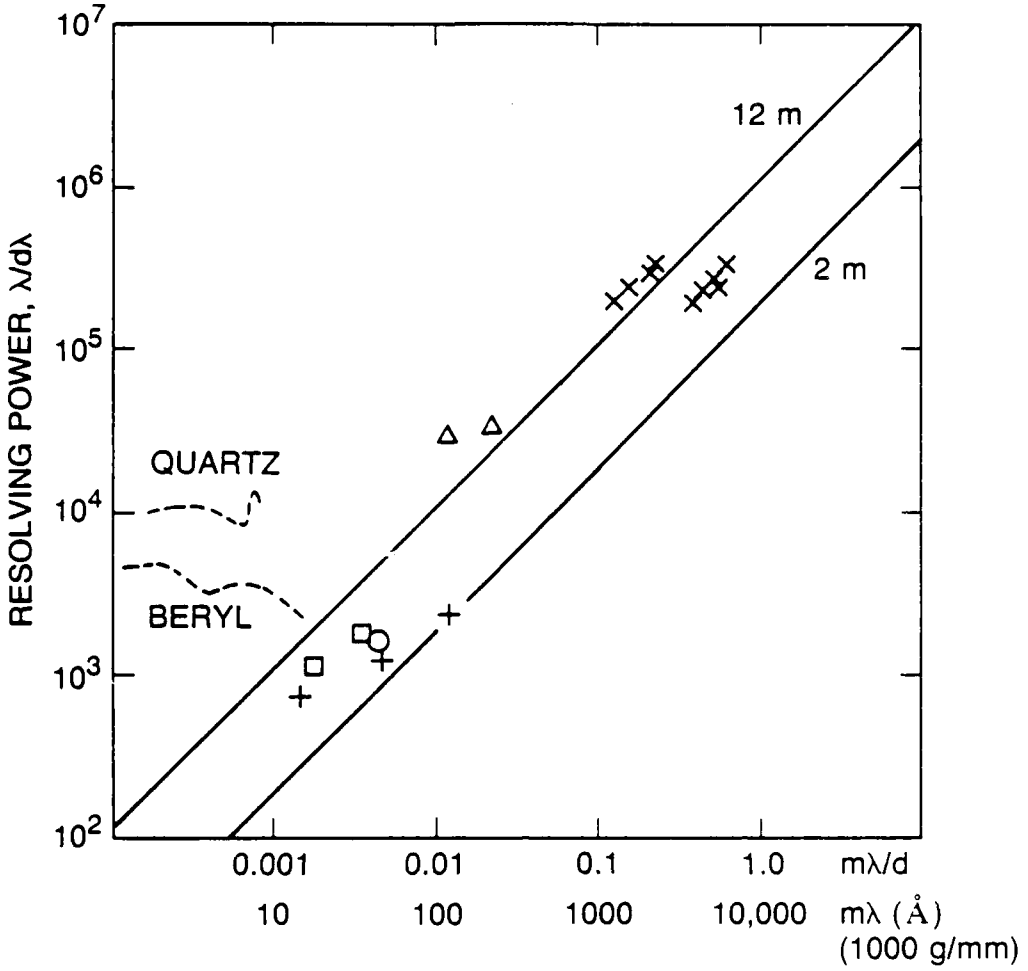

Fig. 4. Resolving power versus mλ/d or mλ with d=1000g/mm. Lines are 1st order resolving powers from Equas. 8i and 10i for Rowland circle spectrometers with 12 and 2 meter diameters, 1000g/mm gratings, and 10μ slits. Points show highest measured resolution UV and soft x-ray grating instruments and crystals: (x) Eagle mount in 3rd and 4th order[28,29]; (Δ) variable line spaced plane grating[30]; (+) plane grating, SX-700,[31]; (circle) toroidal grating[32]; and (box) spherical grating[33]. Dashed lines show Beryl and Quartz crystals. All measurements are 1st order except for the Eagle mount.

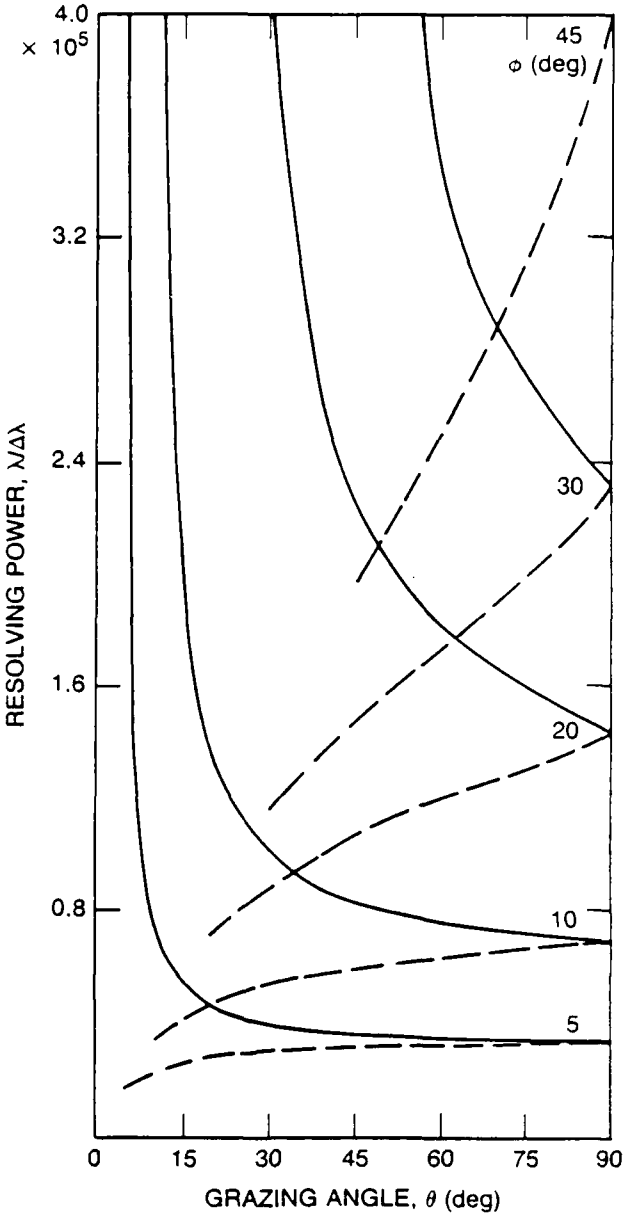

Fig. 5. Resolving power versus facet grazing angle, θ, for on-blaze or multilayer-coated grating spectrometers with fixed focal length design. Fixed slit dispersion (dashed line) and maximum coherent (solid line) resolving powers from Equas. 8ii and 10ii (inside order) are plotted for several blaze angles, ϕ, with $2f_i/s_i = 2f_r/s_r = 4.0 \times 10^5$ (f=10m and s=50μ, for example). Outside order would reverse dashed and solid lines.

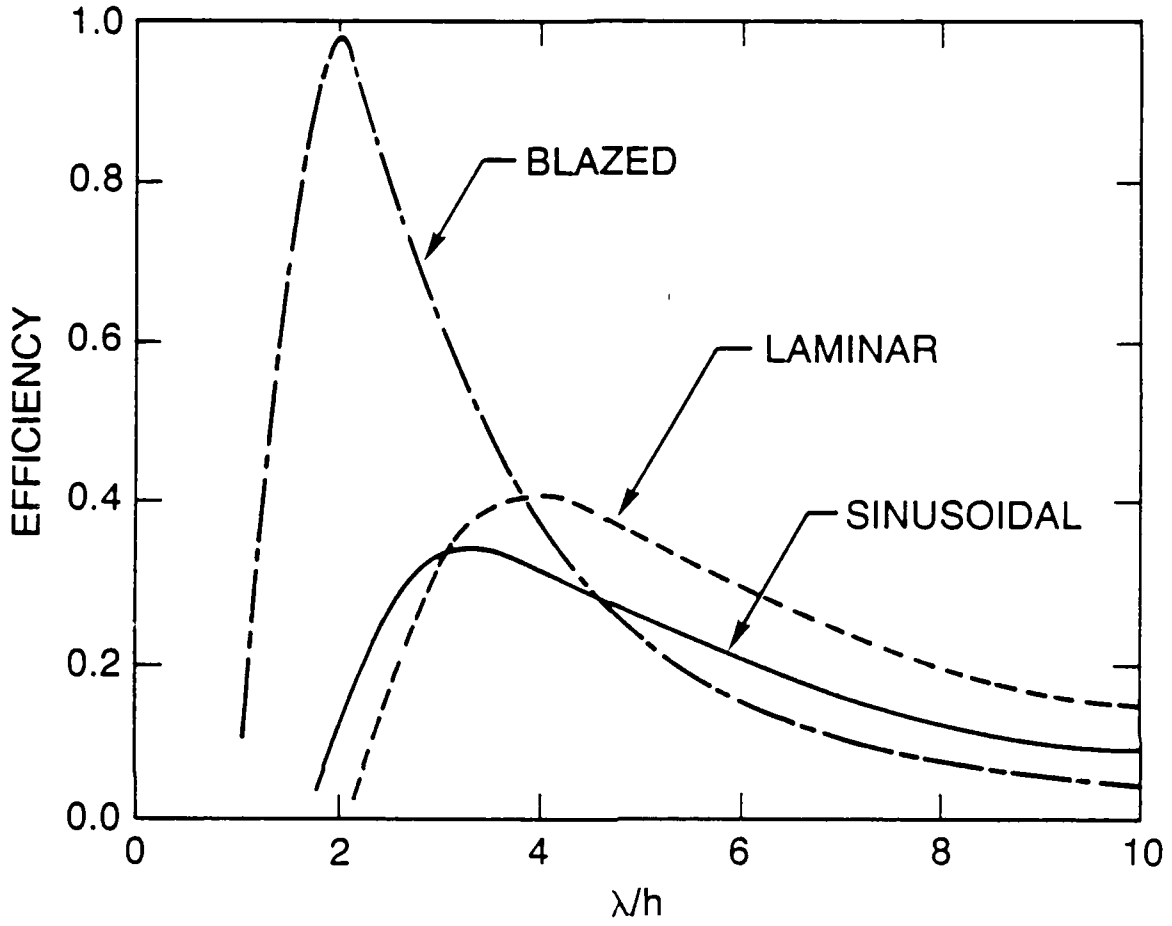

Fig. 6. Grating groove profile efficiency in the scalar regime versus λ/h where h is the groove height for the three standard groove profiles; blazed, laminar, and sinusoidal. Adapted from Vidal et al.[49]

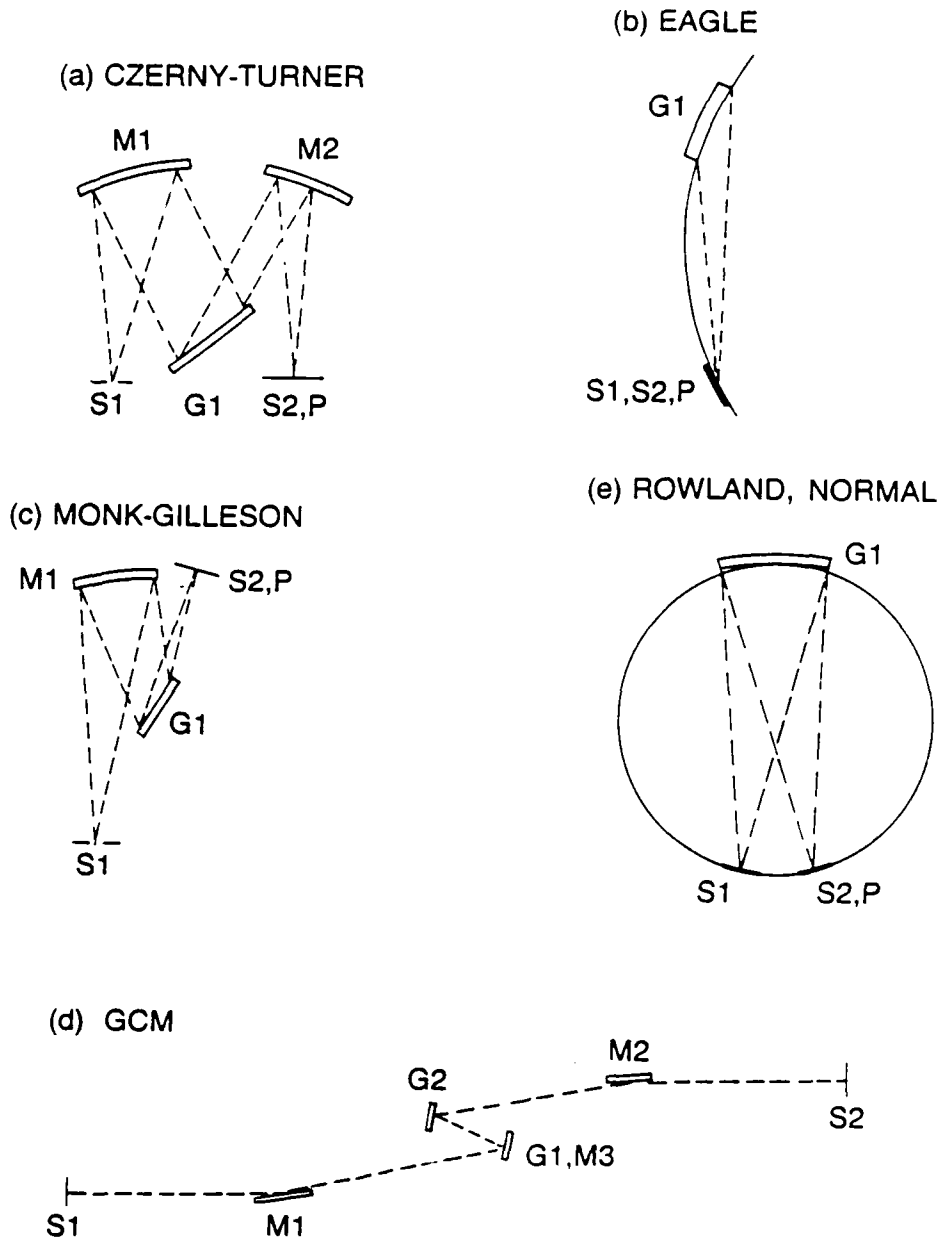

Fig. 7. Mounts for multilayer gratings discussed in the text: (a)Czerny-Turner; (b)Eagle; (c)Monk-Gilleson; (d)Rowland in near normal incidence; and (e)GCM. S1 and S2 are entrance and exit slits; P is a spectrograph plate. M1, M2, and M3 are focussing mirrors; and G1 and G2 are gratings.

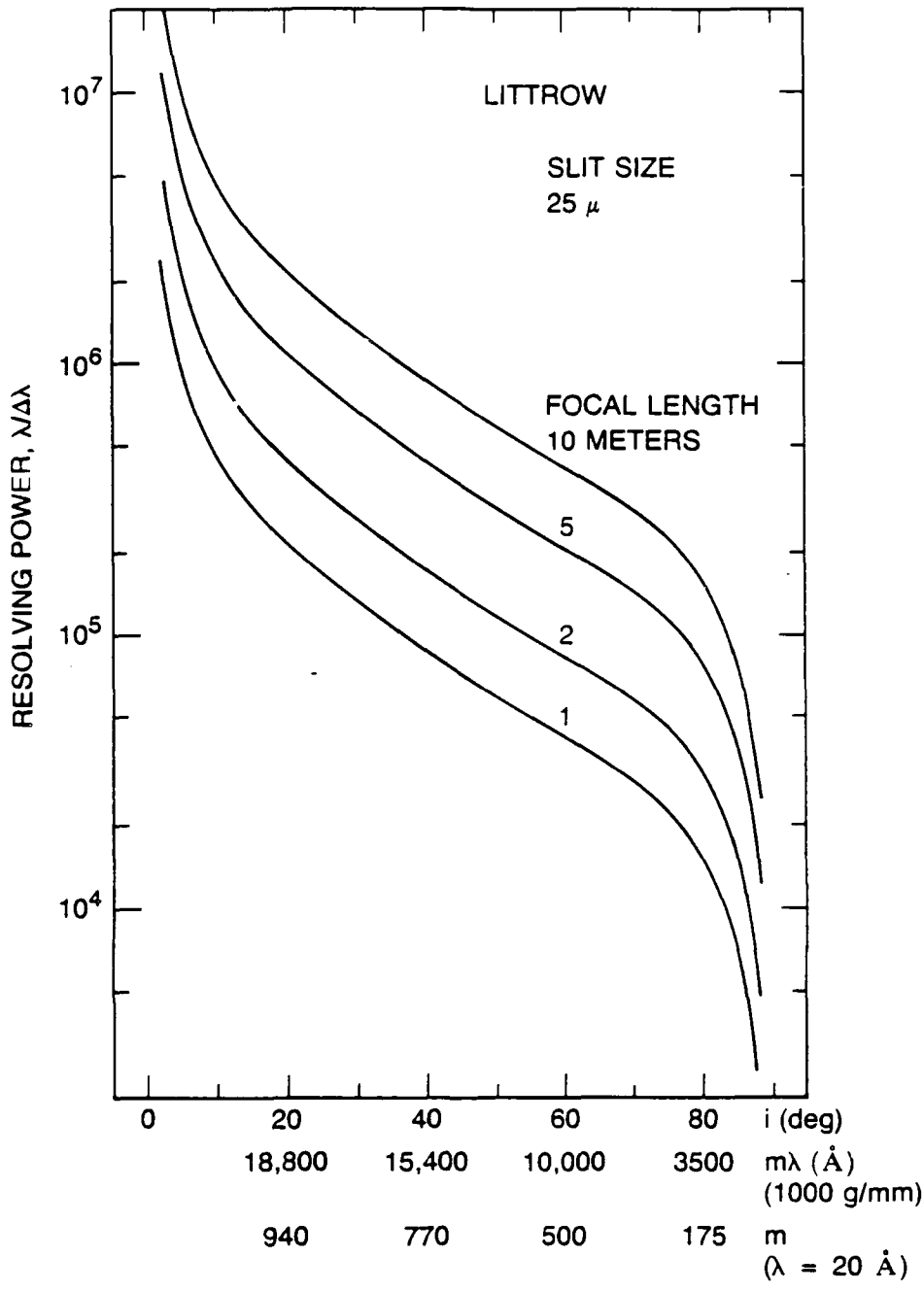

Fig. 8. Resolving power versus grating grazing angle, i, for a Littrow mount with 10, 5, 2, and 1 meter focal lengths to 25μ entrance and exit slits. Order-wavelength product, mλ, is given in Å for a 1000 g/mm grating, and order, m, for operation at λ=20Å.